ORIGINAL PAPER

Andreas Krell · Sigrid B. Schnack-Schiel
David N. Thomas · Gerhard Kattner · Wang Zipan
Gerhard S. Dieckmann

Phytoplankton dynamics in relation to hydrography, nutrients and zooplankton at the onset of sea ice formation in the eastern Weddell Sea (Antarctica)

Abstract The quantitative and qualitative distribution of phytoplankton was investigated along five North–South transects in the eastern Weddell Sea during the transition from late autumn to winter. Relationships with the regional hydrography, progressing sea ice coverage, nutrient distribution and zooplankton are discussed and compared with data from other seasons. To the north of the Antarctic Slope Front (ASF) a remnant temperature minimum layer was found above the primary pycnocline throughout summer. Surface waters had not entirely acquired typical winter characteristics. While temperature was already in the winter range, this was not the case for salinity. Highest biomass of phytoplankton, with the exception of the first transect, was found in the region adjoining the ASF to the north. Absolute chlorophyll a (Chl a) concentrations dropped from 0.35 to 0.19 µg l^{-1}. Nutrient pools exhibited a replenishing tendency. Ammonium concentrations were high (0.75–2 µmol l^{-1}), indicating extensive heterotrophic activity. The phytoplankton in the ASF region was dominated by nanoflagellates, particularly *Phaeocystis* spp.. North of the ASF the abundance of diatoms increased, with *Fragilariopsis* spp., *F. cylindrus* and *Thalassiosira* spp. dominating. Community structure varied both due to hydrographical conditions and the advancing ice edge. The phytoplankton assemblage formed during late autumn were very similar to the ones found in early spring. A POC/PON ratio close to Redfield, decreasing POC concentration and a high phaeophytin/Chl a ratio, as well as a high abundance of mesozooplankton indicated that a strong grazing pressure was exerted on the phytoplankton community. A comparison between primary production (PP) in the water column and the sea ice showed a shift of the major portion of PP into the ice during the period of investigation.

Keywords Weddell Sea · ASF · Hydrography · Phytoplankton · Seasonal change · Community composition · Primary production · Zooplankton

A. Krell (✉) · S. B. Schnack-Schiel · G. Kattner
G. S. Dieckmann
Alfred Wegner Institute for Marine and Polar Research,
Am Handelshafen 12, 27570 Bremerhaven, Germany
E-mail: akrell@awi-bremerhaven.de

D. N. Thomas
School of Ocean Science, University of Wales-Bangor,
Menai Bridge, Anglesey, LL59 5AB, United Kingdom

W. Zipan
2nd Institute of Oceanography, PO Box 1207,
Hangzhou, 310012, Republik of China

Introduction

The southernmost of the circumpolar fronts is the Antarctic Slope Front (ASF), which is identified as a subsurface zone of increased horizontal gradients between most shelf water and deep water parameters such as temperature, salinity and chemical properties. The location of this front is topographically controlled by the Antarctic shelf break (Jacobs 1991; Sokolov 2002 (Fig. 1)). Although well known as a characteristic hydrographic feature of considerable biological significance (Ainley and Jacobs 1981; Wright and van den Enden 2000) our knowledge of this area is still restricted, mainly due to the remote location and pack ice cover which hinders investigations during most of the year.

Only a few studies have been carried to address phytoplankton dynamics in the eastern Weddell Sea during winter (Nöthig et al. 1991), spring (Scharek 1991; Scharek et al. 1994), summer (Nöthig 1988; von Bodungen et al. 1988) and early autumn (Gleitz et al. 1994). However, despite an almost all-year-round coverage, one of the most incisive events in the annual cycle, the onset of sea ice formation, has been omitted. The only published study to date took place after this study, but further to the east at the Greenwich meridian and with
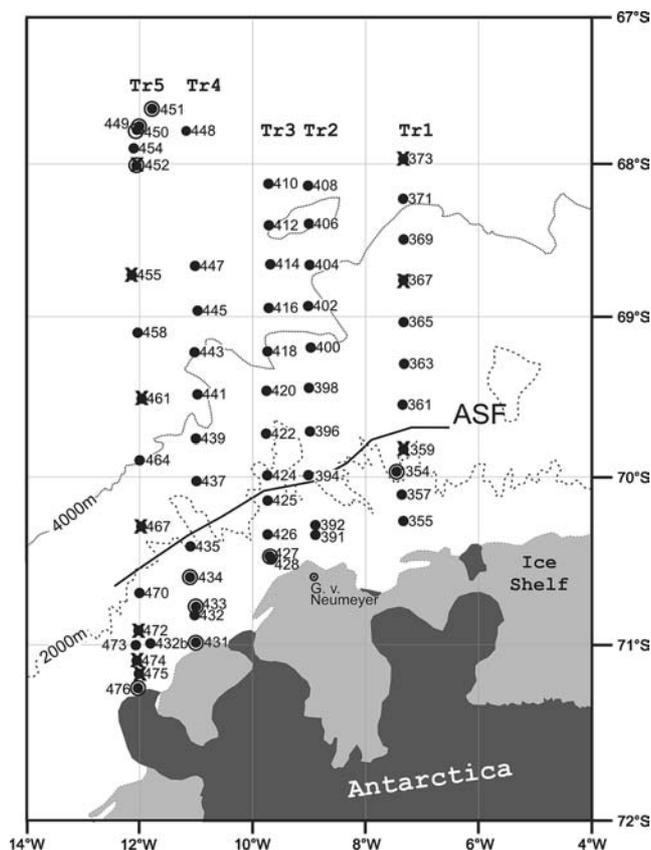
Fig. 1 Station map with locations of the Bio-Rosette casts taken in the Weddell Sea during expedition ANT X/3. Circled stations = either Chl *a* or hydrography data are missing. Crossed stations = zooplankton stations. ASF = Antarctic Slope Front as determined from data obtained in this study

Fig. 2 Stereographic map of sea ice concentration (first year and multiple year ice) from April/May 1992. Box indicates area of investigation. Lines denote 50% concentration determined on specific dates. Calculations are based on brightness temperature data generated by the Special Sensor Microwave/Imager (SSM/I). Data obtained from National Snow and Ice Data Center (1992)

inferior resolution at the ASF (Spiridonov et al. 1996). During the transition between late autumn and winter, changes in the complex hydrographic features at the site of investigation are likely to substantially influence the distribution of phytoplankton both spatially and, in the context of sea ice formation, also temporally. The sampling period described here was marked by rapid sea ice production and hence a rapidly progressing sea ice cover in April 1992 (Fig. 2).

It has become widely accepted that primary production and phytoplankton blooms are mainly determined by the stabilization of the water column (Smetacek and Passow 1990). Whereas this seems to be correct for coastal regions, primary production in oceanic areas of the Southern Ocean seems to be closely linked to the occurrence of fronts (Laubscher et al. 1993; Smetacek et al. 1997). In the area of this investigation both presumptions are important, since it is both a frontal region and in close proximity to the coast and edge of the ice shelf, respectively. Therefore this frontal region may also provide a major contribution in the way of CO_2 drawdown by subsequent sinking of particles (Priddle et al. 1992; Bellerby et al. 2004).

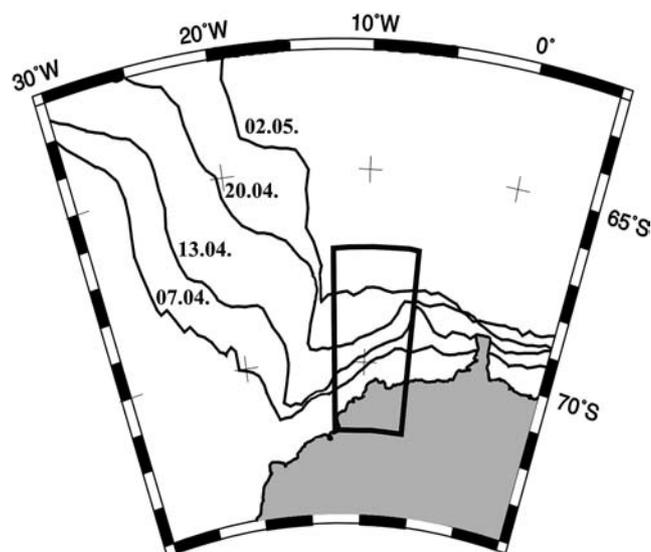This study is aimed to gather further insight into qualitative and quantitative changes in phytoplankton standing stock and underlying processes occurring in the upper water column, both across the ASF and during transition between late autumn and winter. The observed variability is related to potentially responsible physical factors, including water mass distribution, mixed layer depth, currents, ice cover dynamics, nutrient distribution and to a lesser extent grazing pressure. The results complement other seasonal studies and provide a more comprehensive picture of year round processes in the high Antarctic.

Materials and methods

A total of 65 stations were sampled along five oceanographic north–south transects, during cruise ANT X/3 of RV 'Polarstern' between April 7 and 2 May, 1992. The sampling area ranged from 67° 40'S to 71° 20'S and from 7° 40'W to 12° 00'W, covering an area of approximately 200000 km^2 (Fig.1). The transects are labelled according to their accomplishment from east to west; Tr1 (7° 40'W), Tr2 (9° 00'W), Tr3 (9° 40'W), Tr4 (11° 00'W) and Tr5 (12° 00'W), respectively.

Data on the light regime were obtained from Dower et al. (1996). To follow the large-scale development of sea ice cover, sea ice concentration data obtained from the National Snow and Ice Data Center (1992) were used.

Conductivity, temperature and depth (CTD) profiles were obtained with a sensor-rosette sampler combination, consisting of a CTD-unit (ME98) equipped with twelve 15 l Niskin bottles. CTD casts were performed down to 500 m. Bottles for water samples were usually triggered at the following standard depths: 0, 10, 20, 30,

50, 70, 100, 125, 150, 200, 250 and 500 m. CTD sensors were calibrated by the manufacturer to an accuracy in temperature of 0.02 K, pressure of 0,25% and conductivity of 0.025 mScm^{-1}. Because of shallow depths of the CTD casts (< 500 m) the temperature rise due to adiabatic compression is negligible. Therefore temperature, that is, in situ temperature is considered equivalent to potential temperature θ.

The term Antarctic Coastal Current refers both to the current associated with the ASF and the fast narrow current along the Antarctic coast (the front of the ice shelf), since in the investigation area the shelf is very narrow and distinction between currents not feasible. Investigations on vertical structure (< 500 m), horizontal circulation patterns and water mass characteristics (Table 1) to determine temporal and/or spatial changes were performed along three transects Tr1, Tr3 and Tr5.

Analysis of inorganic nutrients (nitrate, nitrite, phosphate and silicate) were carried out on board using a Technicon AII AutoAnalyzer within a few hours after sampling (Kattner and Becker 1991). Measurement of ammonium was carried out manually using a method for small (5 ml) sample volumes modified after Grasshoff et al. (1983).

Particulate organic carbon/nitrogen (POC/PON) samples were taken at all depths up to station 420 and subsequently only sporadically. Subsamples for POC and PON determinations were filtered through precombusted (500°C, 12 h) GF/F filters (Whatmann). Filters were frozen immediately and stored at −27°C for later analysis. Prior to determinations, filters were acidified with four drops of 1N hydrochloric acid, and dried overnight at 60°C. They were then transferred into tin vials and analysed using a Perkin Elmer CHN analyser calibrated with acetanilide standards.

For Chl *a* and phaeophytin, 2 l subsamples were filtered through 25 mm Whatman GF/F filters, extracted in 90% acetone and measured on board using a Turner Designs Fluorometer. Phaeophytin was measured after the addition of three drops 5% 1N HCl. Chl *a* and phaeophytin concentrations were calculated from fluorescence readings after the method of Evans et al. (1987).

Phytoplankton samples were only taken on Tr2, excluding station 391 and 392 (Fig.1). Subsamples for species composition of 100 ml were filled into bottles and fixed with hexamine-buffered formaldehyde (final conc. 2%). These samples were stored in the dark at ≈15°C and counted within 12 months. Microscopic analysis was carried out using a Zeiss IM 35 microscope. Counting was performed after Utermöhl (1958) at 100 to 400x magnification using phase contrast. Large diatoms were counted on the entire bottom, species having cell sizes smaller than 23 μm only on strips.

Zooplankton samples were only collected on Tr1 and Tr5 and treated as described by Schnack-Schiel et al. (1998) and complemented by the counts of euphausids. For this study data of the uppermost multinet layer (0–70/120 m depth) were used and standardized to a depth of 70 m. Only stations where both Chl *a* and mesozooplankton data are available were evaluated.

Results

Environmental data

The sampling period was marked by a considerable decrease in day length from more than 10 h to less than 4 h. Thus, daily integrated irradiance declined from 9.5 molm^{-2} d^{-1} to ≈0.3 molm^{-2} d^{-1} during the course of the expedition. The 1% light depth based upon Secchi disk measurements ranged from 62 m to 84 m (Dower et al. 1996).

Rapid sea ice formation took place during the sampling period, not as a uniform front but was influenced by local hydrographical factors with different stages of sea ice formation as described by Lange et al. (1989). The embayment visible in the sea ice cover on 02 May (Fig.2) along the coast was the remainder of a larger wedge-shaped lead. It could be clearly observed in satellite images of the preceding weeks.

Most obvious during this transitional period was the fact that the ASF was characterized not only by subsurface gradients but by temperature and salinity gradients, recognizable at the surface (Fig. 3a, b). As conditions approached the typical winter situation (Fig. 3c), the ASF was limited to the reported presence of subsurface gradients (Jacobs 1991; Fahrbach et al. 1992). The beginning formation of the Winter Mixed Layer (WML) was detected as a northwards progressing surface frontal zone associated with the northward movement of sea ice, most evident in the temperature section between stations 369 and 361 at Tr1 (Fig. 3a) and between stations 416 and 420 at Tr3 (Fig. 3b). The final section along 12°00'W resembled typical winter conditions. The sea ice cover and the WML extended across the entire transect (Fig. 3c). The pycnocline in the oceanic regime on Tr1 and Tr3 was around 70 m and slightly shallower (50 m) in front of the ice edge (st. 416) on Tr3. On Tr5 it had dropped to 100 m.

Table 1 Potential temperature θ, salinity S and oxygen O$_2$ characteristics for water masses in the eastern Weddell Sea

Water mass	Θ (°C)	S	O$_2$(ml/l)
Winter Water (WW)	$-2.0 \le \Theta \le -1.6$	$34.40 \le S \le 34.52$	$6.6 \le O_2 \le 6.9$
Warm Deep Water (WDW)	$0.0 \le \Theta \le 0.8$	$34.60 \le S \le 34.76$	$4.3 \le O_2 \le 4.9$
Eastern Shelf Water (ESW)	$-2.0 \le \Theta \le -1.6$	$34.28 \le S \le 34.44$	$7.2 \le O_2 \le 7.4$

Water mass nomenclature used is based on the definitions of Carmack (1974), Foster and Carmack (1976) and Carmack and Foster (1977)

Fig. 3 Isotherms down to 500 m perpendicular to the coast on **a** Tr1, **b** Tr3 and **c** Tr5, respectively. Shaded areas represent shelf, numbers above graph CTD stations

The ASF showed different trends during the study period: a two step dipping of the isolines was a characteristic feature on Tr1 and Tr3. There, an initial sharp dip in the thermocline coincided with the location of the MIZ. The primary frontal break occurred further south between station 424 and 425, a feature best seen in the temperature section (Fig. 3b). The step-like dipping of the 0°C isotherm was not evident at Tr5. The subsurface near coastal dip of the 0°C isotherm coincided with the core of the Coastal Current, and the strong density gradient which drives the baroclinic component of this current system was clearly reflected at the location of the front.

As visible in the Temperature/Salinity (T/S) plots (Fig. 4), coastal stations (open labels) were generally marked by low temperatures throughout the water column down to 500 m. In contrast considerable changes in surface temperature were recorded at the oceanic stations. On Tr1 (Fig. 4a) the northernmost station (373) showed high temperature values around −0.98°C down

to 50 m (not obvious since almost all values in Fig. 4a are superimposed) resembling summer values above a strong pycnocline (Fig. 3a), and indicating that a low amount of vertical mixing was occurring. This profile was typical for stations north of the frontal zone. Further south, summer water was capped by a colder (−1.5 −−1.8°C), slightly fresher new WML. Although not visible in the isopleth plots (Fig. 3) due to the vertical resolution, at 70 m temperatures increased to −0.965°C, resembling a remnant summer temperature-maximum (t-max) layer relative to the waters above and even below. Underneath this layer a previous winter temperature minimum layer existed between 80 m and 100 m depth, again indicative of low vertical mixing. Further south on the shelf, the water column reached consistently low temperatures around −1.84°C. This trend could also be seen at Tr3 (Fig. 4b). The remnant temperature maximum layer at station 418 at 50 m and 70 m is clearly visible. A slight increase in salinity at station 418 and station 424 already indicated the
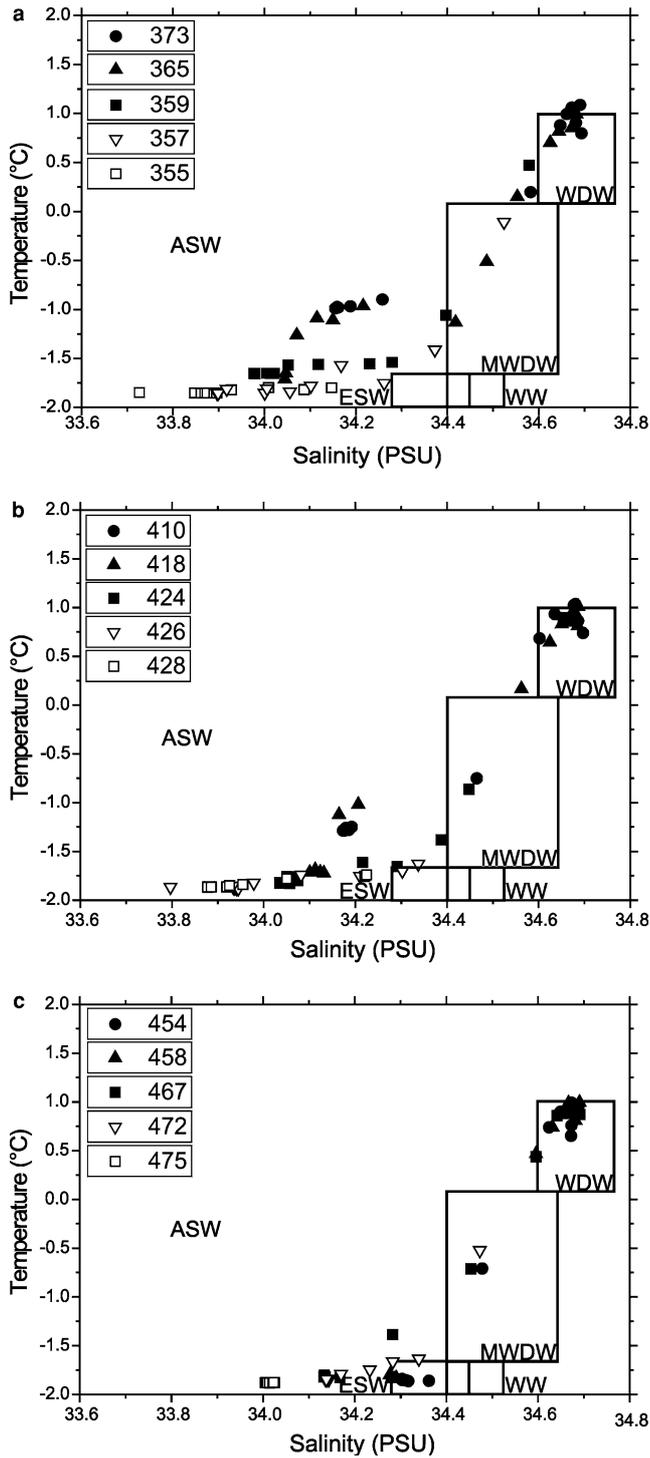
Fig. 4 T/S-diagrams of **a** Tr1, **b** Tr3 and **c** Tr5. Only T/S-values of standard depths are depicted plus an additional point at 400 m. Oceanic stations are labelled with solid, coastal ones with open symbols

beginning of sea ice formation and concomitant brine release. At Tr5 (Fig. 4c) it is evident that the entire upper water column of all oceanic stations had cooled, reaching Winter Water (WW) values, whereas with progressing sea ice cover and subsequent brine release,

salinity increased significantly but had not yet attained WW values. In the permanent thermocline and slightly below, Modified Warm Deep Water (MWDW), a water mass with characteristics between ASW and WDW was detected.

Nutrients and biological parameters

The ASF was also seen in the nutrient data with values on the shelf similar to surface values (< 70 m) in oceanic regions. In almost all cases the nutricline exhibited good agreement with the pycnocline. Since nitrite concentrations were continuously low (< 0.33 µmol l^{-1}) they are not further considered. Apart from ammonium, nutrient concentrations in the surface water were substantially lower than those from below the nutricline. Nitrate, phosphate and silica concentrations showed an increasing trend towards the west (Fig.5). Nitrate concentration in surface waters increased westward from values around 25 µmol l^{-1} to above 27 µmol l^{-1}. Silica ranged from ≈ 54 on Tr1 to more than 62 µmol l^{-1} on Tr5. Phosphate concentrations varied from 1.65 in the east to above 1.9 µmol l^{-1} on the last transect. Phosphate data reached a high peak (2.38 µmol l^{-1}) on Tr4 station 437 situated directly above the ASF compared to surrounding surface values. This peak corresponded with an elevated ammonium concentration of 5.47 µmol l^{-1}. Generally, ammonium exhibited reverse trends to other nutrient data with elevated values on the shelf and in surface waters. The ammonium nutricline was not well pronounced in the last two transects.

Particulate organic carbon/nitrogen (C/N) ratios varied over a considerable range with a general mean of 5.95 (sd $= \pm 1.02$), although consistent with the ratio, which is 5.68 on a weight basis (Redfield et al. 1963). A more detailed look reveals that the C/N ratio in the uppermost 50 m (this depth was chosen in contrast to Chl a, since data suggested that remineralization had already started in the deeper surface mixed layer above the pycnocline) was lower($\bar{x} = 5.59, \text{sd} = \pm 0.75$) and more consistent compared to depths below 50 m ($\bar{x} = 6.25, \text{sd} = \pm 1.46$). Comparing single transects, which is difficult since data of Tr4 and Tr5 are limited, it reveals an increase in the C/N ratio from Tr1 ($\bar{x} = 5.37$) to Tr2 ($\bar{x} = 6.1$) and a subsequent decline of $\bar{x} = 5.79$ to $\bar{x} = 5.01$ from Tr3 to Tr5. This correlated with the decreasing trend of Chl a values, but a comparison within single transects shows elevated C/N ratios on the shelf, contrary to Chl a data. An elevated C/N ratio of 9.84 was found at station 367, concomitant with the Chl a peak, as were high POC concentrations between 79.66 µg l^{-1} and 136.86 µg l^{-1} at 20 m to 70 m.

Chl a values in the surface layer (< 70 m) were low in the entire area of observation (max. 19.8 mg m^{-2}, stat. 396) (Fig.6a), with an actual mean concentrations of $\bar{x} = 0.15 \mu g l^{-1}$ (sd $= \pm 0.065$, n $= 326$). Higher values of 0.35 µg l^{-1} were found at station 396 from 0–50 m
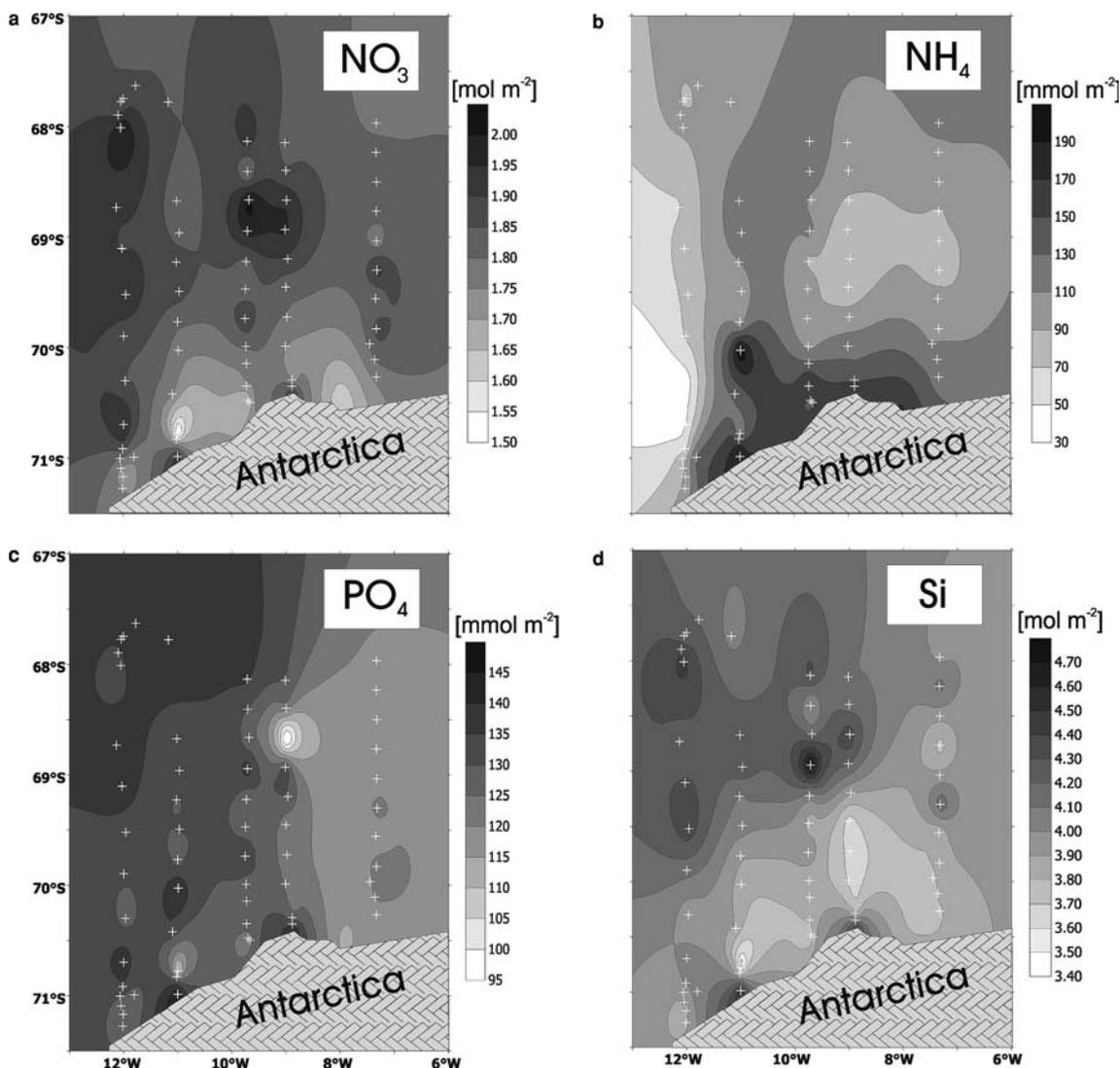
Fig. 5 Concentration of **a** NO₃, **b** NH₄, **c** PO₄ and **d** Si integrated down to 70 m

and an exceptional peak of 0.40 µg l^{-1} at station 367 at 70 m depth (Fig.6a, b) associated with a warm core eddy. It is evident that the ASF marks a distinct boundary with respect to the distribution of Chl *a*. Values of Chl *a* south of the ASF were below 0.15 µg l^{-1} throughout the entire water column (Fig. 6b). Highest values of Chl *a* were found at 0–50 m depth just north of the ASF except on Tr1 with a decreasing trend towards the west (Fig.6a). Incorporation of phytoplankton into newly formed grease ice did occur, since higher Chl *a* values than in the adjacent water column were found in six grease ice samples (Chl *a* conc. $\bar{x} = 0.66\,\mu g l^{-1}$ sd = ±0.17) (Dower et al. 1996).

To account for prevailing hydrographical conditions data are further on considered as coastal (south of the ASF) and oceanic (north of the ASF), the latter divided into depths above (< 70 m) and below the pycnocline. Photosynthetic biomass on an areal basis clearly showed a decreasing trend in all realms (Fig. 6a). A significant

reduction of Chl *a* in the oceanic surface layer from 15.02 mg m^{-2} to 8.41 mg m^{-2} between Tr1and Tr5 was calculated.

The carbon/Chl *a* ratio in the oceanic realm above the pycnocline was very high throughout the observation area, ranging between 133 and 671 (n = 143). The average ratio of single transects (< 70 m) ranged between 272 and 333 showing little variability.

Total range of Phaeo/Chl *a* ratios was between 0.13 and 3.22. Values of the entire study area in the surface layer (< 70 m) were very consistent at 0.64 ±0.1. Values below the pycnocline and on the shelf (1.16 ±0.48 and 0.86 ±0.25) were higher but did not exhibit any tendency.

Phytoplankton community structure

Along Tr2 the cell numbers were generally low with a maximum of 1.5× 10^6 cells l^{-1} at station 396; 30 m (Fig. 7). A separation into two regimes was obvious, one dominated by flagellates to the south of station 398

Fig. 6 Chlorophyll a **a** biomass
[mg Chl a m^{-2}] integrated
down to 70 m and
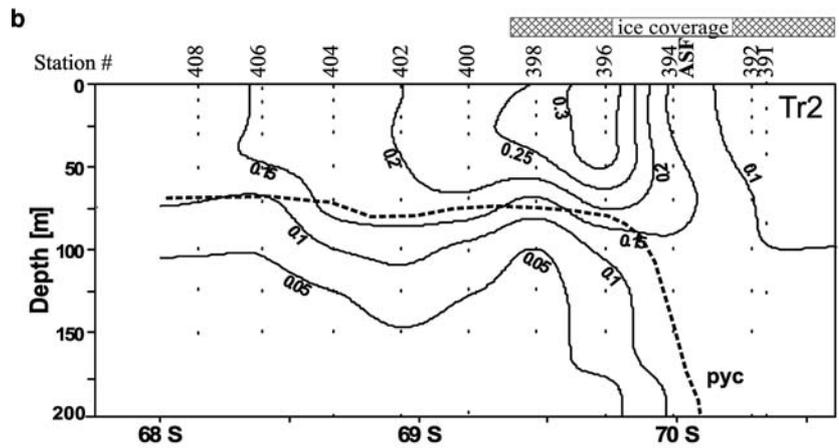**b** distribution [µg l^{-1}]
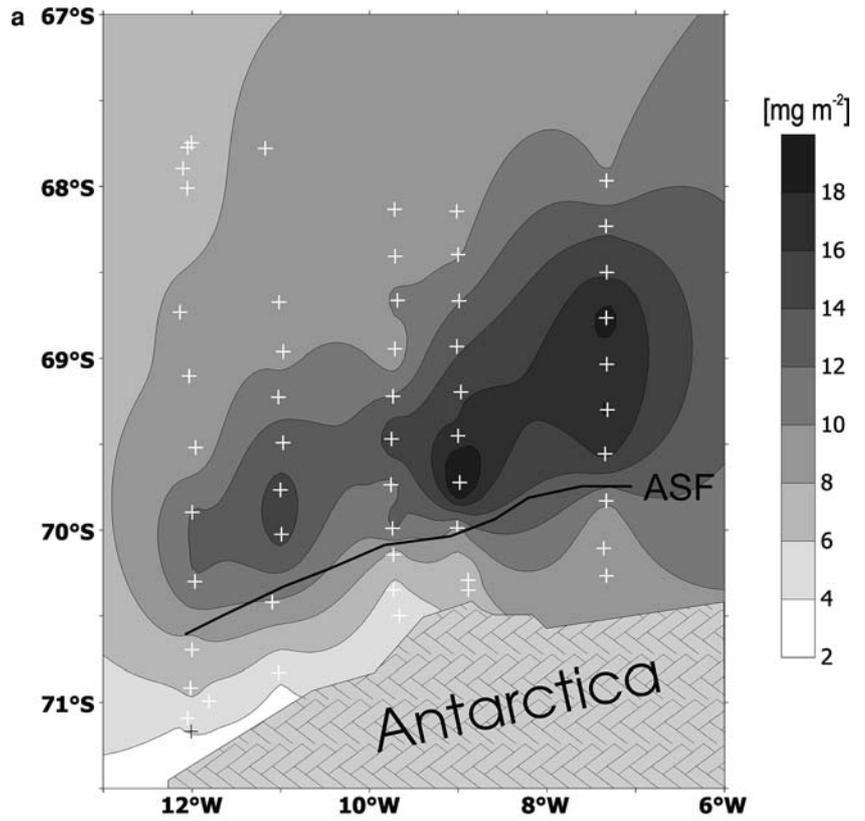on Tr2, pyc = pycnocline

Fig. 7 Total cell numbers (10^6
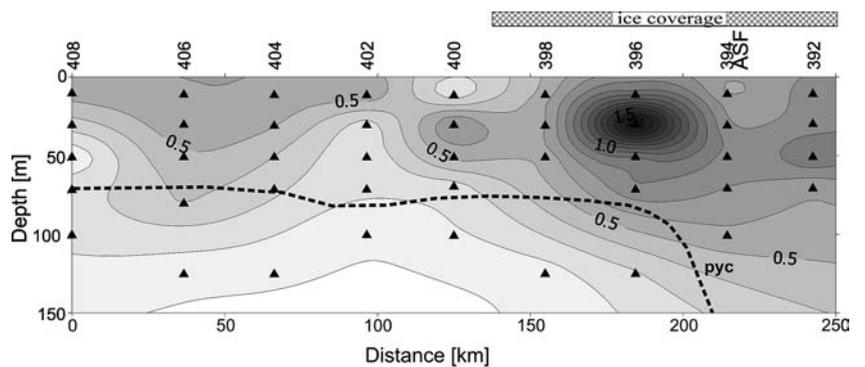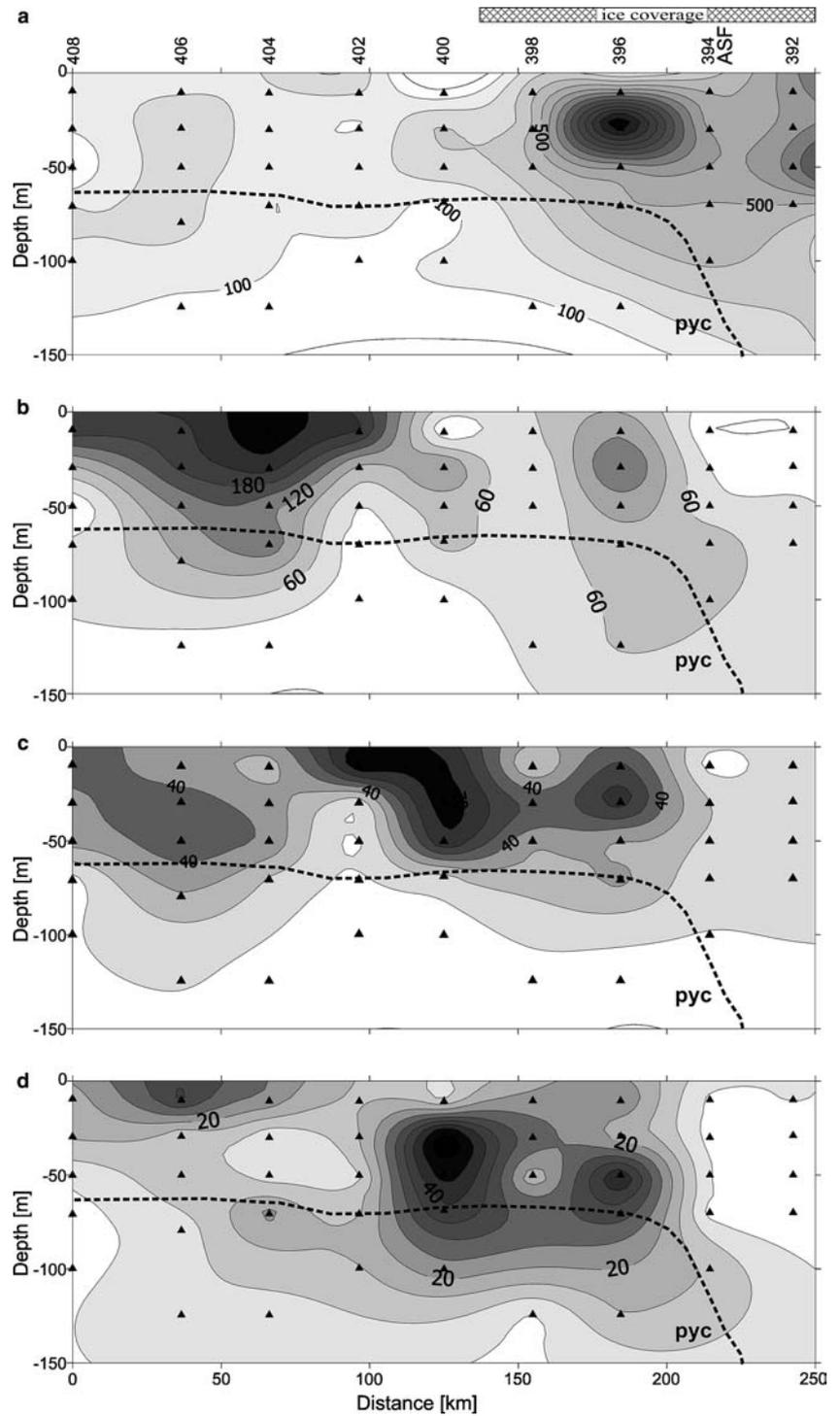cells l^{-1}) along Tr2, pyc =
pycnocline

Fig. 8 Distribution of selected phytoplankton taxa **a** *Phaeocystis* spp. colony cells as well as motile stages and small flagellates (< 10 μm). Contribution of *Phaeocystis* spp. amounts to 25–50%, **b** Fragilariopsis cylindrus, **c** *Thalassiosira* spp. and **d** *Fragilariopsis kerguelensis* along Tr2 in cells l^{-1}

(Fig. 8a), while north of it diatoms were more abundant (Fig. 8b–d). The peak at station 396 was due to the high abundance of *Phaeocystis* spp. and small (< 10 μm) flagellates (Fig. 8a) making up more than 2/3 of total cell numbers. Although dinoflagellates and small flagellates were counted they were not identified as being auto-trophic or heterotrophic. Diatoms, especially *Fragilariopsis cylindrus* (Fig. 8b) and *Thalassiosira* spp. (Fig. 8c)

also contributed to this peak, though at lower cell numbers. However, diatoms generally occurred further north, for example, at station 400, 30 m and at the surface of stations 404/406. Species with elevated cell numbers in this region were the already mentioned *F. cylindrus* and *Thalassiosira* spp., as well as *F. kerguelensis* (Fig. 8c). High numbers (5–10× 10^3 cells l^{-1}) of large (< 38 μm) empty *Asteromphalus* spp. frustrules
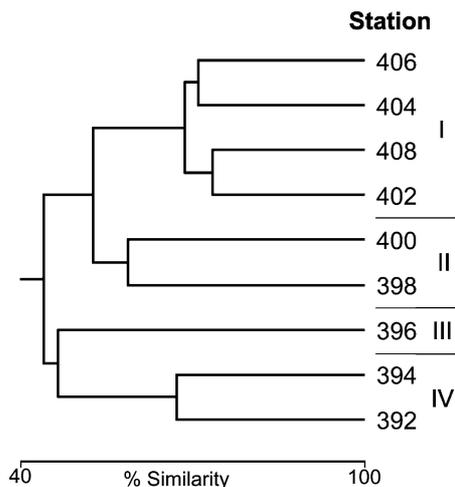
Station

Fig. 9 Dendrogram of sampled stations resulting from Bray and Curtis 1957) cluster analysis

were found, with a similar distribution to that of *F. kerguelensis*. The diatom assemblage was dominated by pennate species, being four times more abundant than centric species. Despite the late season, no shift of the plankton community towards a resting assemblage was observed, and with the exception of a few spores of *Eucampia antarctica* no resting stages were found. At the MIZ situated between stations 398 and 400, cell numbers were lowest at the surface.

Cluster analysis after Bray and Curtis (1957) based upon cell counts, taking even into account different size classes of one species, revealed four classes at the 55% similarity level, which form two clusters at the 45% similarity level (Fig. 9). The latter corresponds to the separation between stations on the shelf and the front and subsequently oceanic stations. The branching off of station 396 at a low similarity level compared to class IV emphasizes the exceptional conditions in the front also reflected by high Chl *a* values at this station. The separation into class I and II which the cluster analysis exhibited, can be related to stations influenced by sea ice formation and foregoing cooling of the water column (class II), whereas the fairly homogenous class I reflects remnant oceanic summer conditions.

Zooplankton

Mean mesozooplankton biomass in the uppermost 70 m (Fig.10), comprising copepods and euphausids amounted to 985 mgC m^{-2} on Tr1 and 722 mgC m^{-2} on Tr5, which are in turn 240% and 325% of mean phytoplankton carbon biomass. Contribution of euphausids to the overall mesozooplankton biomass was less than 5%, except for one station on Tr1 and Tr2 where it was 15%. Copepod community was, at most stations dominated by Calanoida, equally followed by Oncaea and Oithona.

Discussion

Hydrography

Since sampling was performed at different sites it is important to assess if variations observed in the data were due to geographic variability, that is, spatial differences or if they reflect continuous processes occurring in the water column, that is, temporal changes. Progression of sampling during the expedition was in the direction of main currents from east to west, covering a distance of 520 km ($\equiv$ 52×10^6 cm) between the first and the last transect (Fig.1). Since the sampling period took 25 days ($\equiv$ 2.16× 10^6 s), a current velocity of 24.1 cms^{-1} would mean that sampling was carried out more or less in the same water body. Long-time current measurements and ADCP data indicate average speed of the current core situated above the upper continental slope in the range of 15 cms^{-1} to 53 cms^{-1} centering around 25 cms^{-1} (Fahrbach et al. 1992; Heywood et al. 1998; Schröder and Fahrbach 1999). The findings show high current velocities in the ASF, slightly lower ones on the shelf and lowest speeds further offshore. Therefore it is most likely that samples taken in the southern part of the investigation area mainly come from the same co-migrating water volume. Hence differences evident in measured data in the ASF region and on the shelf more probably reflect temporal changes occurring in the same water body rather than sampling of different water bodies. However, further offshore the effects of spatial variability maybe more profound.

Hydrography in the oceanic region of the study area is characterized by a two layer surface system still resembling summer conditions. The topmost layer, warmed due to solar heating is separated through a seasonal pycnocline from underlying remnant WW with higher salinity and lower temperature (not visible in Fig. 3 because of low resolution). This WW layer is expected to erode in thickness during summer, but this data indicates that even in late autumn the layer still exists, preventing deep vertical mixing, and enabling better growth conditions for phytoplankton. During the study period, surface waters had neither reached oceanic WW, nor coastal Eastern Shelf Water (ESW) properties reported for this region (Fahrbach et al. 1992). Despite the fact that temperature had already dropped to within the WW and ESW range, salinity values were too low.

Although coastal stations were already covered by newly formed sea ice, water properties had not changed markedly indicating that not enough brine had drained out by then and/or the process of meltwater formation had not yet completely ceased. The measured delay of sea ice formation (Fig. 2) in the ASF region is a feature also observed by Heywood et al. (1998). They attributed this prolonged maintenance of open water to relatively warmer waters being advected from the northeast. Another possible explanation is the erosion of the t-max layer (Fig. 3) lying at shallow depths in this region via

advective heat transport in the vicinity of the ASF. However, ice free conditions in the region north of the ASF were thereby prolonged for about 10 days. The observed hydrographical features have the following consequences for phytoplankton dynamics:

– The homogeneous water column on the shelf impedes in situ build up of phytoplankton biomass by deep vertical mixing. But onshore Ekman transport enabled by easterly winds can cause oceanic waters to cross the ASF (Fahrbach et al. 1992) and thereby import phytoplankton into the water body on the shelf.
– The stratification of the water column north of the ASF favours the growth of phytoplankton, but with the erosion of the seasonal pycnocline stratification is destroyed in autumn or early winter.
– The advection of warmer waters from the east (Heywood et al. 1998) and the erosion of the t-max layer retard ice growth in this region, enabling, though only for a period of a few days, better conditions for phytoplankton growth.

Biological parameters

The highest Chl a peak at station 367 (Fig. 7) was most probably caused by a cyclonic eddy type current which was cut tangentially. The core of this eddy was clearly detectable on a parallel eXpendable BathyThermograph (XBT) transect at 8°W (data not shown in this report). Relating Chl a and nutrient data measured within the investigation period to data obtained during other seasons (Table 2), they plainly reflect the transitional period between late autumn and winter. The observed decrease of Chl a fits well into the annual cycle: Although Chl a concentrations of summer and post-bloom conditions reported by Gleitz et al. (1994) are considerably higher, winter values are an order of magnitude lower.

The already increasing nutrient concentrations, especially the repletion of the phosphate pool and the exceptionally high ammonium concentration indicate rapid recycling and replenishing of nutrient pools during late autumn. Although ammonium provides a preferable nitrogen source for phytoplankton and in contrast to nitrate shows no negative temperature dependence in uptake (Reay et al. 2001), the high values suggest that it cannot be used due to insufficient light availability.

Phytoplankton community structure

Sea ice is a major factor influencing the observed phytoplankton distribution pattern. The observed low cell numbers between stations 398 and 400 (Fig. 7), possibly indicate strong incorporation of phytoplankton into newly forming sea ice. Pancake coverage was 80% and wind speeds around 8–10.7 m s⁻¹ prevailed, indicating turbulent conditions of ice formation. This suggests that all three mechanisms of phytoplankton incorporation, scavenging, nucleation (Weeks and Ackley 1982) and wave induced pumping (Weissenberger et al. 1992), were relevant. Whereas the effect of wave induced pumping is negligible under the already existing ice cover, harvesting and nucleation may still take place. This is supported by the fact, that south of this region, highest cell numbers were found at depths around 30 m, whereas north of the MIZ phytoplankton was most abundant at the surface. If compared to Chl a values (Fig. 6b) which showed a gradual decrease from highest values at station 396 concurrent with cell number peak, towards the northern end of the transect, cell numbers were also decreasing. But whereas the decrease in cell numbers amounted to roughly 66% this was opposed by a decrease of only approximately 50% in Chl a concentration. This indicates that diatoms, despite their lower cell numbers, were contributing significantly to the Chl a pool, due to a larger cell size and a different Chl a content per cell.

Although dense phytoplankton blooms in the Southern Ocean MIZ have been reported in earlier studies (Smith and Nelson 1986; Smetacek et al. 1990), recent findings have failed to confirm stability induced phytoplankton blooms associated with the MIZ (Bathmann et al. 1997). The position of hydrographical features like fronts appeared to determine at least in part the location of these blooms, rather than the location of the retreating ice edge (Boyd et al. 1995; Pollard et al. 1995). The observed distribution pattern almost resembled the same structure which was found at the MIZ during spring transition in October/December several degrees further to the north. Scharek et al. (1994) found a similar Phaeocystis and flagellate dominated community in the MIZ at 58°S in October with relatively low diatom concentrations, although consisting of different species. Garrison et al. (1993) also encountered an identical structured system at comparable low biomass in the MIZ of the western Weddell Sea in early austral

Table 2 Range of Chl a and nutrient values in the upper mixed layer of the eastern Weddell Sea

Parameter	Oct/Nov	Dec/Jan	Feb/Mar	Apr/May	Jun/Jul
Chl a [µg l⁻¹]	0.05–0.15 [a] 0.01 [e]	0.1–0.19 [e]	0.1–0.8 [b] < 1.0 [b]	1.6–2.3 [b] 0.1–0.4 [c]	0.01–0.05 [d]
NO₃[µmol l⁻¹]	30.5–31.5 [e]	31.0 [e]	23.8–31.5 [b]	< 17 [b] 24.8–27.7 [c]	
PO₄[µmol l⁻¹]	1.95–2.05 [e]	2.05–2.15 [e]	1.8–2.3 [b]	< 1.5 [b] 1.65–1.95 [c]	
NH₄[µmol l⁻¹]	0.1–0.7(< 0.07) [e] < 0.2 [f]			0.75–2 [c]	
Si[µmol l⁻¹]			54.9–76.5 [b]	< 50 [b] 54–62 [c]	

Sources: [a]Nöthig unpubl, [b]Gleitz et al. (1994), [c]present report, [d]Spiridonov et al. (1996), [e]Scharek (1991) () = shelf, f Nöthig et al. (1991)

winter. About 1 month later Spiridonov et al. (1996) recorded phytoplankton cell numbers of only 200×10^3 cells l^{-1} in the coastal current. Nanoflagellates were about 100×10^3 cells l^{-1} with *Phaeocystis* accounting for 50% as in this report. Diatom abundance was dominated by *F. cylindrus*. These findings agree well with our results. Although total cell numbers had decreased considerably and the importance of nanoflagellates in relation to diatoms had decreased, the composition of the phytoplankton community did not change substantially. Furthermore, Scharek et al. (1994) found nanoflagellate (mainly *Phaeocystis*) and dinoflagellate dominated phytoplankton communities with low diatom concentrations in late winter (October). It appears that the community structure of overwintering phytoplankton is to a large extent already determined in late autumn.

A further explanation for the observed community structure is directly coupled with the hydrography of the ASF, or fronts in general. It has been observed at tidal mixing fronts that diatoms grow better in well-stratified waters, whereas flagellate growth exceeds that of diatoms in deeper mixed waters in close proximity to fronts (Arrigo et al. 1999). This is consistent with findings of this report, that diatoms were more abundant in the more stratified oceanic region north of station 400, whereas the flagellate peak occurred in deeper mixed waters (Fig. 8a) adjacent to the ASF. This distribution pattern was also observed and related to hydrography by Wright and van den Enden (2000) at the ASF further to the east. Similar flagellate dominated phytoplankton communities were found in summer (January/February) in the shelf and slope region (Nöthig 1988; Estrada and Delgado 1989). This leads to the assumption, that the phytoplankton community in this region of the ASF, apart from occasional diatom blooms, might be flagellate dominated, at least in terms of cell numbers the whole year round, especially at the ASF and on the shelf where a high degree of vertical mixing occurs. These conclusions are strongly supported by previous findings of Smetacek et al. (1990), who also described the Antarctic pelagic phytoplankton community as being dominated by nanoflagellates and small pennate diatoms, especially during winter.
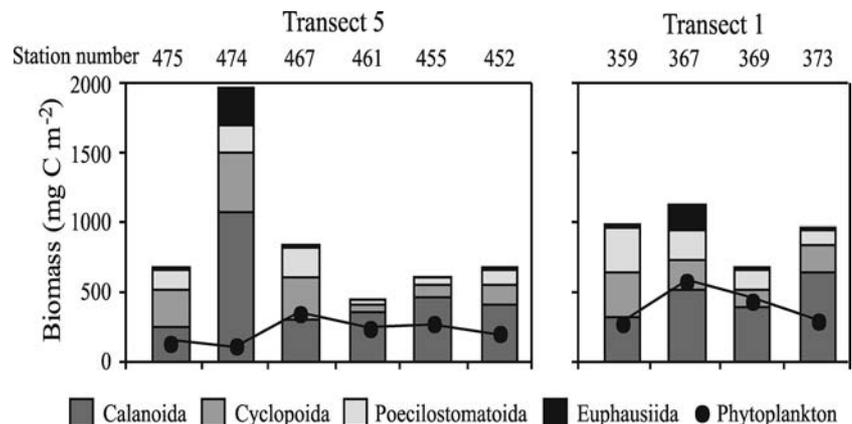
However, the cluster analysis (Fig. 10) reveals a distinct difference in similarity, between the homogeneous class I in the oceanic ice free realm and the MIZ (class II) and closed pack ice region (classes III + IV). This illustrates a clear imprint of ice conditions on the community structure. Thus phytoplankton community structure is firstly influenced by the frontal conditions at the ASF, but a primary dependence on ice coverage results during the transition period between late autumn and winter. However, ice coverage ultimately is also influenced by hydrographical conditions. Arrigo et al. (1999) found, that the draw-down of both carbon dioxide (CO_2) and nitrate per mole of phosphate and the rate of new production by diatoms are much lower than that measured for *Phaeocystis antarctica*. The observed community structure at the ASF would therefore favour the draw-down of CO_2. In contrast to the dominance of nanoflagellates in the water column, diatoms dominated in the closed ice sheet, accounting for 80% of total phytoplankton cell numbers (Gleitz and Thomas 1993).

Zooplankton

Phytoplankton blooms as observed by Gleitz et al. (1994) in late February might be fostered by comparatively low mesozooplankton abundance. Calanoid copepods reached their highest annual biomass on the shelf and frontal region in April/May with numbers of 300 and 900 Ind m^{-3} in the topmost 200 m (Schiel 1998). This fact is further supported by the exceptionally high ammonium concentrations (Table 2) found, indicating high heterotrophic activity (Biggs 1982). Though the phaeo/Chla ratio could also indicate a poor physiological state of phytoplankton cells, the low amount of biomass compared to the high nutrient concentrations (Table 2), as well as temperature effects on phytoplankton physiology (Tilzer and Dubinsky 1987) do not corroborate this. Therefore in late autumn phytoplankton biomass accumulation might not only be limited by

Fig. 10 Integrated (< 70 m) phytoplankton and mesozooplankton biomass in [mgCm^{-2}] at **a** Tr1 and **b** Tr5, assumed C/Chla ratio $= 30$

deteriorating light conditions, but to a much greater extent by increased grazing pressure.

Since no data are available, the influence of bacteria and protozooplankton cannot be discussed, although data by Gleitz et al. (1994), who found 50–100% of primary production consumed by bacteria, suggest that a substantial fraction of primary production might be removed by bacteria.

A crude estimation of primary productivity is attempted, mainly based on literature data. Dower et al. (1996) calculated primary production rates of 15.6 – 41.5 mgC m^{-2} d^{-1} in the same area integrated down to the critical depth. This can be assumed to be a very conservative estimate, since they used a photocompensation irradiance of 5 μmol m^{-2} s^{-1}, whereas values of 1 μmol m^{-2} s^{-1} or even less are more appropriate (Mock and Kroon 2002). Gleitz and Thomas (1993) reported increasing production rates based upon ^{13}C incorporation technique from the open water to closed pack ice of 1.2 – 36 mgC m^{-2} d^{-1} . Although carbon uptake rate did not exceed 4.8 mgC mgChla^{-1} d^{-1} in closed pack ice, the increase in cell concentration overcompensated for the decrease in photosynthetic capacity. This results in a maximum areal primary production in closed pack ice of 24 mgC m^{-2} d^{-1} Gleitz and Thomas (1993). Assuming that primary production in the open water declines within the observed range by Dower et al. (1996) this loss can at least be partially compensated by primary production in the ice. Thus, this region may be able to sustain a primary production capacity of up to 40 mgC m^{-2} d^{-1} far into late autumn despite decreasing light conditions. The main production site therefore progresses from the water column to sea ice.

To evaluate the stability of the ecological system with regard to two trophic levels, that is, phytoplankton and mesozooplankton, a comparison of standing stock and productivity related to grazing pressure is attempted. The C/Chl a ratios measured in this study are to our knowledge the highest reported values for polar regions so far. Hegseth and von Quillfeldt (2002) found similar ratios (366 to 453) in February 1997 just south of the study area. They also attributed these high ratios to large amounts of non-phytoplankton carbon, indicative of retention system with high grazing activity. Recent findings of the C/Chl a ratio in sea ice containing different amounts of biomass were in the same order of magnitude as values calculated for this study but still at the lower limit (Kattner et al. 2004). These high ratios would suggest that sources contributing to the POC pool analysed here may be other than phytoplankton, for example, bacteria, detritus, exopolymeric substances and faecal pellets. Using these ratios as a basis to calculate phytoplankton standing stock would most probably not reflect the situation in the water column at this time of the year and thus result in unrealistic values. Values in the range of 75 for summer phytoplankton (Swadling et al. 1997) and 22–12 for shade adapted phytoplankton during the spring season (Hegseth 1997) were reported for polar regions. A median C/Chl a ratio of 30 was therefore assumed, in order to estimate phytoplankton carbon standing stock (Fig. 10). Given the range mentioned above, a value in the lower range is justified for the study presented here, since the study period was characterized by declining light levels and adaptation of phytoplankton is retarded. However, even with a C/Chl a ratio of 60, phytoplankton biomass would still be below that of mesozooplankton. In addition production rates of the remaining phytoplankton community are assumed to be decreasing due to the deteriorating abiotic conditions. Regardless of the absolute rate of primary production, due to the above- mentioned shift of primary production towards the ice, this biomass is not readily accessible to zooplankton. Thus it can be concluded that the high Antarctic ecosystem at this point of the year is transitional and not sustainable.

Conclusion

Previous investigations of the biological processes and productivity along the ASF are sparse and have been carried out mainly during summer season. This report reveals the complex interactions between hydrography, biology and sea ice at the ASF during late autumn. There is evidence that the phytoplankton community structure is determined by the mixing regime at the ASF as well as the proceeding ice edge. The community structure of over-wintering phytoplankton is apparently nanoflagellate dominated and already determined in late autumn. Together with previous investigations (Nöthig 1988; Estrada and Delgado 1989, Smetacek et al. 1990) this indicates that this nanoflagellate dominated phytoplankton structure possibly prevails the whole year round. Phytoplankton growth north of the ASF is favoured by stratification in summer, but onshore Ekmann transport causes parts of this stock to cross the ASF south and evenly disperse in the water column on the shelf. Balancing of primary production shows that the main production site changes from the water column to the ice, by which a high production rate appears to be maintained into late autumn. Hence, with regard to the season the ASF region is able to substantially contribute to the fixation of carbon in the South Eastern Weddell Sea late into the austral autumn. However, high abundances of copepods, the phae/Chl a ratio and the C/N ratio suggest that exceptionally high grazing is exerted on phytoplankton during late autumn. The question is weather production rate and the standing stock of phytoplankton is able to provide sufficient food supply to the high mesozooplankton stock abundant at this time of the year. Findings of Jacobs (1991) who identified the ASF as a region of high primary production and concentration of predatory species can be confirmed by the present report.

References

Ainley DG, Jacobs SJ (1981) Sea-bird affinities for ocean and ice boundaries in the Antarctic. Deep Sea Res 28A:1173–1185

Arrigo KR, Robinson DH, Worthen DL, Dunbar RB, DiTullio GR, VanWoert M, Lizotte MP (1999) Phytoplankton community structure and the drawdown of nutrients and CO_2 in the Southern Ocean. Science 283:365–367

Bathmann UV, Scharek R, Klaas C, Dubischar CD, Smetacek V (1997) Spring development of phytoplankton biomass and composition in major water masses of the Atlantic sector of the Southern Ocean. Deep Sea Research Part II: Topical Studies in Oceanography 44:51–67

Bellerby RGJ, Hoppema M, Fahrbach E, de Baar HJW, Stoll MHCMHC (2004) Interannual controls on Weddell Sea surface water fCO2 during the autumn-winter transition phase. Deep Sea Research Part I: Oceanographic Research Papers 51:793–808

Biggs DC (1982) Zooplankton excretion and NH_4 cycling in near-surface waters of the Southern Ocean 1. Ross Sea, austral summer 1977–1978. Polar Biology 1:55–67

von Bodungen B, Nöthig EM, Sui Q (1988) New production of phytoplankton and sedimentation during summer 1985 in the southeastern Weddell Sea. Comp Biochem Physiol B: Comp Biochem 90B:475–487

Boyd PW, Robinson C, Savidge GJ, Williams PJ (1995) Water colomn and sea ice primary production during austral spring in the Bellingshausen Sea. Deep Sea Research Part II: Topical Studies in Oceanography 42:1177–1200

Bray JR, Curtis JT (1957) An ordination of the upland forest communities of southern Wisconsin. Ecological Monographs 27:325–349

Carmack E (1974) A quantitative charactarization of water masses in the Weddell Sea during summer. Deep Sea Res 21:431–443

Carmack E, Foster TD (1977) Water masses and circulation in the Weddell Sea. In: Dunbar M (ed) Polar Oceans. Arktic Institut of North America, Calgary, Canada, pp 151–166

Dower KM, Lucas MI, Phillips R, Dieckmann G, Robinson DH (1996) Phytoplankton biomass, P-I relationships and primary production in the Weddell Sea, Antarctica, during the austral autumn. Polar Biology 16:41–52

Estrada M, Delgado M (1989) Summer phytoplankton distributions in the Weddell Sea. Polar Biology 10:441–449

Evans CA, O'Reilly JE, Thomas JP (1987) A handbook for the measurement of chlorophyll a and primary production. Biological Investigations Of Marine Antarctic Systems and Stocks (BIOMASS). Texas A & M University, College Station, Texas

Fahrbach E, Rohardt G, Krause G (1992) The Antarctic Coastal Current in the southeastern Weddell Sea. Polar Biology 12:171–182

Foster TD, Carmack EC (1976) Frontal zone mixing and Antarctic Bottom Water formation in the southern Weddell Sea. Deep Sea Res 23:301–317

Garrison DL, Buck KR, Gowing MM (1993) Winter plankton assemblage in the ice edge zone of the Weddell and Scotia Seas: Composition, biomass and spatial distributions. Deep Sea Research Part I: Oceanographic Research Papers 40:311–338

Gleitz M, Thomas DN (1993) Variation in phytoplankton standing stock, chemical composition and physiology during sea-ice formation in the southeastern Weddell Sea, Antarctica. J Exp Mar Bio Ecol 173:211–230

Gleitz M, Bathmann UV, Lochte K (1994) Build-up and decline of summer phytoplankton biomass in the eastern Weddell Sea, Antarctica. Polar Biology 14:413–422

Grasshoff K, Ehrhardt M, Kremling K (1983) Methods of sea water analysis. Verlag Chemie, Weinheim

Hegseth EN (1997) Phytoplankton of the Barents Sea – the end of a growth season. Polar Biology 17:235–241

Hegseth EN, von Quillfeldt CH (2002) Low phytoplankton biomass and ice algal blooms in the Weddell Sea during the ice-filled summer of 1997. Antarctic Science 14:231–243

Heywood KJ, Locarnini RA, Frew RD, Dennis PF, King BA (1998) Transport and water masses of the Antarctic Slope Front system in the eastern Weddell Sea. In: Jacobs SS, Weiss RF (eds) Ocean, ice, and atmosphere: interactions at the antarctic continental margin, vol. 75, pp 203–214

Jacobs SS (1991) On the nature and significance of the Antarctic Slope. Front. Mar Chem 35:9–24

Kattner G, Becker H (1991) Nutrients and organic nitrogenous compounds in the marginal ice zone of the Fram Strait. J Mar Syst 2:385–394

Kattner G, Thomas DN, Haas C, Kennedy H, Dieckmann GS (2004) Surface ice and gap layers in Antarctic sea ice: highly productive habitats. Mar Ecol Prog Ser 277:1–12

Lange MA, Ackley SF, Wadhams P, Dieckmann G, Eicken H (1989) Developement of sea ice in the Weddell Sea. Ann Glaciol 12:92–96

Laubscher RK, Perissinotto R, McQuaid CD (1993) Phytoplankton production and biomass at frontal zones in the Atlantic sector of the Southern Ocean. Polar Biology 13:471–481

Mock T, Kroon BMA (2002) Photosynthetic energy conversion under extreme conditions–II: the significance of lipids under light limited growth in Antarctic sea ice diatoms. Phytochemistry 61:53–60

National Snow and Ice Data Center (1992) DMSP SSM/I brightness temperatures and sea ice concentration grids for the polar regions, 1992. National Snow and Ice Data Center, Distributed Active Archive Center Digital data available from nsidc@kryos.colorado.edu

Nöthig EM (1988) On the ecology of the phytoplankton in the southeastern Weddell Sea (Antarctica) in January/February 1985. Rep Polar Res 53:118

Nöthig EM, Bathmann U, Jennings JC, Fahrbach E, Gradinger R, Gordon LI, Makarov R (1991) Regional relationships between biological and hydrographical properties in the Weddell Gyre in late austral winter 1989. Mar Chem 35:325–336

Pollard RT, Read JF, Allen JT, Griffiths G, Morrison AI (1995) On the physical structure of a front in the Bellingshausen Sea. Deep Sea Research Part II: Topical Studies in Oceanography 42:955–982

Priddle J, Smetacek V, Bathmann U (1992) Antarctic marine primary production biogeochemical carbon cycle and climate change. Philosophical Transactions of the Royal Society of London, Series B 338:289–297

Reay D, Priddle J, Nedwell D, Whitehouse M, Ellis-Evans J, Deubert C, Connelly D (2001) Regulation by low temperature of phytoplankton growth and nutrient uptake in the Southern Ocean. Mar Ecol Prog Ser 219:51–64

Redfield A, Ketchum B, Richard F (1963) The influence of organisms on the composition of sea water. In: Hill M (ed) The sea, pp 26–77

Scharek R (1991) Development of phytoplankton during the late-winter/spring transition in the eastern Weddell Sea (Antarctica). Rep Polar Res 94:195

Scharek R, Smetacek V, Fahrbach E, Gordon LI, Rohardt G, Moore S (1994) The transition from winter to early spring in the eastern Weddell Sea, Antarctica: Plankton biomass and composition in relation to hydrography and nutrients. Deep Sea Research Part I: Oceanographic Research Papers 41:441–449

Schiel SB (1998) Die calanoiden Copepoden des östlichen Weddellmeeres, Antarktis: Saisonales Vorkommen und Lebenszyklen dominater Arten. In: Habilitationsschrift der Mathematisch-Naturwissenschaftlichen Fakultät der Christian-Albrechts Universität Kiel, p 227

Schnack-Schiel SB, Hagen W, Mizdalski E (1998) Seasonal carbon distribution of copepods in the eastern Weddell Sea. J Mar Syst 17:305–311

Schröder M, Fahrbach E (1999) On the structure and the transport of the eastern Weddell Gyre. Deep Sea Research Part II: Topical Studies in Oceanography 46:501–527

Smetacek V, Passow U (1990) Spring bloom initiation and Sverdrup's critical-depth model. Limnol Oceanogr 35:228–234

Smetacek V, Scharek R, Nöthig EM (1990) Seasonal and regional variation in the pelagial and its relationship to the life history cycle of krill. In: Kerry K and Hempel G (eds) Antarctic ecosystems: Ecologycal change and conservation. Springer Verlag, Berlin, pp 103–114

Smetacek V, De Baar HJW, Bathmann UV, Lochte K, Van Der Loeff MMR (1997) Ecology and biogeochemistry of the Antarctic Circumpolar Current during austral spring: a summary of Southern Ocean JGOFS cruise ANT X/6 of R.V. Polarstern. Deep Sea Research Part II: Topical Studies in Oceanography 44:1–21

Smith WO, Nelson DM (1986) Importance of ice-edge production in the Southern Ocean. Bio Sci 36:251–257

Sokolov S, Rintoul SR (2002) Structure of Southern Ocean fronts at 140[deg]E. J Mar Syst 37:151–184

Spiridonov VA, Noethig EM, Schroeder M, Wisotzki A (1996) The onset of biological winter in the eastern Weddell Gyre (Antarctica) planktonic community. J Mar Syst 9:211–230

Swadling KM, Gibson JAE, Ritz DA, Nichols PD, Hughes DE (1997) Grazing of phytoplankton by copepods in eastern Antarctic coastal waters. Mar Biol 128:39–48

Tilzer MM, Dubinsky Z (1987) Effects of temperature and day length on the mass balance of Antarctic phytoplankton. Polar Biology 7:35–42

Utermöhl H (1958) Zur Vervollkommnung der quantitativen Phytoplankton-Methodik. Mitt int Ver theor angew Limnol 9:1–38

Weeks WF, Ackley SF (1982) The growth, structure and properties of sea ice. CRREL Monogr 82(1):130

Weissenberger J, Dieckmann G, Gradinger R, Spindler M (1992) Sea ice: a cast technique to examine and analyze brine pockets and channel structure. Limnol Oceanogr 37:179–183

Wright SW, van den Enden RL (2000) Phytoplankton community structure and stocks in the East Antarctic marginal ice zone (BROKE survey, January-March 1996) determined by CHEMTAX analysis of HPLC pigment signatures. Deep Sea Research Part II: Top Stud Oceanogra 47:2363–2400